Combined-Levitation-and-Propulsion Control of SLIM Maglev Vehicle on Flexible Guideway

Yoshida, Kinjiro
Department of Electrical and Electronic Systems Engineering, Faculty of Information Science and Electrical Engineering, Kyushu University, Kyushu University

Yoshida, Takashi
Department of Electrical and Electronic Systems Engineering, Graduate School of Information Science and Electrical Engineering, Kyushu University : Graduate Student

Noda, Kuni
Department of Electrical and Electronic Systems Engineering, Graduate School of Information Science and Electrical Engineering, Kyushu University : Graduate Student

https://doi.org/10.15017/1515813

出版情報：九州大学大学院システム情報科学紀要. 8 (1), pp.25-30, 2003-03-26. 九州大学大学院システム情報科学研究院

Combined-Levitation-and-Propulsion Control of SLIM Maglev Vehicle on Flexible Guideway

Kinjiro YOSHIDA*, Takashi YOSHIDA** and Kuni NODA**

(Received December 13, 2002)

Abstract: Based on the decoupled control method of attractive-normal and thrust forces in a single-sided linear induction motor (SLIM), a compact combined-levitation-and-propulsion SLIM Maglev vehicle can be realized without any additional levitation magnet. In a Maglev system, if the distance between two pillars is long compared with the moving vehicle, a vibration of the guideway is one of the most important problems. This paper presents a combined-levitation-and-propulsion control system with considering the guideway vibration in Maglev vehicle realized by SLIM only. For stable levitation and propulsion, estimated airgap length has been calculated from the measured airgap length by gapsensor and attractive-normal force has been analyzed by finite element method (FEM). Experimental results show that the vehicle can be propelled and levitated stably for the flexible guideway.

Keywords: SLIM, Decoupled control, Estimated airgap length, Attractive-normal force, Flexible guideway

1. Introduction

Compared with linear synchronous motor (LSM), LIM has much simpler construction, its maintenance is easier and the cost is much lower. LIM can be applied to transportation system as a no-contacting driving source, combined with another independent levitation system.[1),2)] But because the normal force of SLIM varies widely from repulsive to attractive forces with the vehicle speed and slip-frequency, this force is generally seldom utilized in transportation systems and its effect is always restrained as small as possible. On the other hand, combined-levitation-and-propulsion SLIM Maglev vehicle which is used in this study is based on a unified concept of machine principle, in which combined magnetic levitation-and-propulsion using only one linear mo-

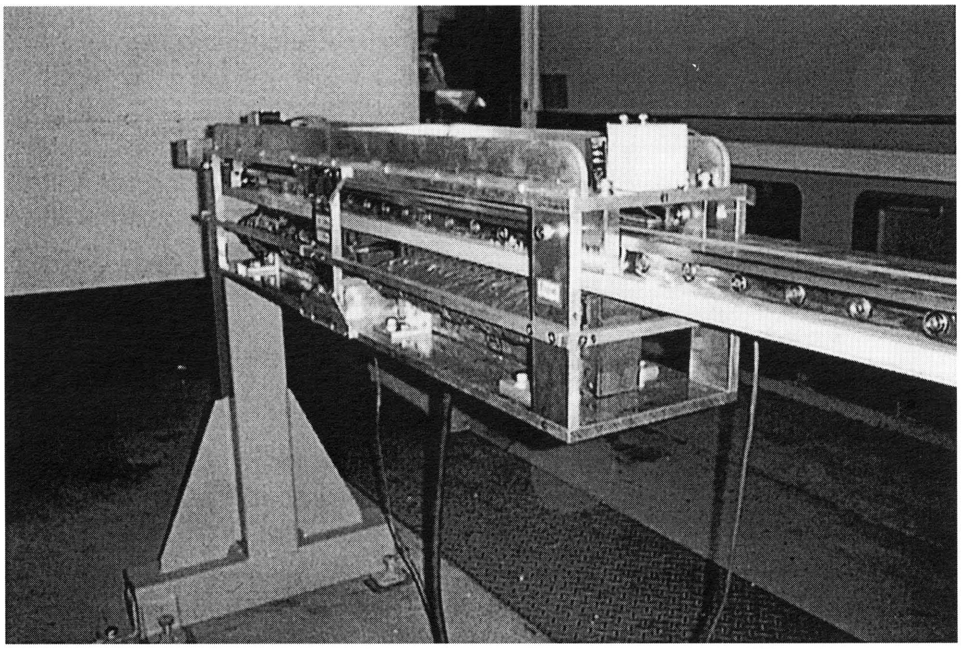

Fig. 1 SLIM experimental Maglev vehicle

* Department of Electrical and Electronic Systems Engineering
** Department of Electrical and Electronic Systems Engineering, Graduate Student

tor has been proposed as a compact system without any additional magnets for levitation.[3] Controlled-repulsive LSM Maglev vehicles have been designed and simulated for feasibility study.[4),5] A decoupled control method of lift and thrust forces has been proposed and effectively used.[6] Marine express (ME) 03 has been realized successfully.[7]

Controlled-attractive SLIM Maglev vehicle has been proposed and experimented based on a decoupled control method of attractive-normal and thrust forces.[8] The decoupled control method of attractive-normal and thrust forces is derived from the analytical formulas for normal and thrust forces in the SLIM with secondary back-iron.[9] Based on this method, the attractive-normal force suspends and the thrust force propels the vehicle simultaneously, a very compact and low-cost combined levitation-and-propulsion Maglev vehicle system is implemented with SLIM only. Moreover in most of the Maglev vehicle system with elevated guideway, the longer the distance between two pillars of the guideway is, the lower its manufacturing cost is.

We have already succeeded in a combined-levitation-and-propulsion control of the SLIM experimental Maglev vehicle using the half length of the guideway which is made by supporting its center.[10),11] But to control the vehicle by making full use of the guideway, the vibration of the guideway is so serious that an excellent adaptive control system must be considered for the vibration.[12]

This paper presents a combined-levitation-and-propulsion control system taking into account the vibration of the guideway in the SLIM Maglev vehicle. Experimental results show that the vehicle can be levitated and propelled simultaneously on the vibrating guideway.

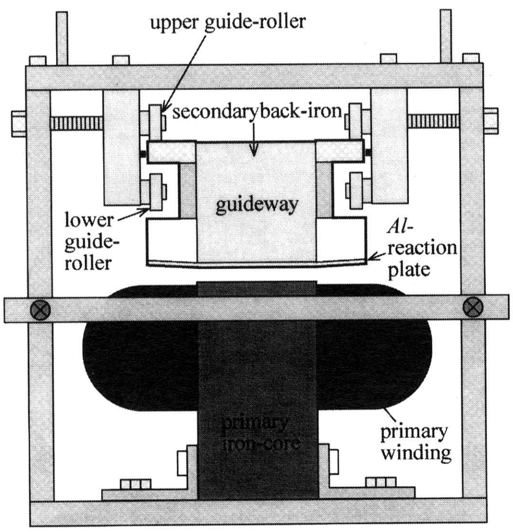

Fig. 2 Transverse cross-section of SLIM experimental Maglev vehicle

Table 1 Specifications of SLIM

Item	Symbol	Value
Number of phase	m	3
Number of pole	p	6
Pole pitch	τ	51mm
Width of primary iron core	h	50mm
Number of slots per pole per phase	q	1
Turns per phase	N_{ph}	300
Winding coefficient	k_{w1}	1.0
Thickness of secondary back-iron	d_1	50mm
Thickness of secondary aluminum	d_2	2.0mm

2. SLIM Maglev Vehicle

Figure 1 shows a SLIM experimental Maglev vehicle. The vehicle is designed and manufactured, which runs along the 3-m-long linear motor guideway in our Laboratory. The vehicle with two independent primaries mounted straight-line at the front and the rear on board is 96 cm in length and about 42 kg in weight. Guideway consists of aluminum reaction plate of 2 mm and back-iron block of 5 cm in thickness and width. **Table 1** shows the specifications of the SLIM. The vehicle is levitated and propelled by only a pair of primary and secondary conductor. The attractive-normal force is used to levitate the vehicle and the thrust force to propel the vehicle without coupling between these two forces.

Figure 2 shows a cross-section of the SLIM experimental Maglev vehicle. It is 19 cm in height and width. In **Fig. 2**, when upper guide-rollers contact with the guideway, the airgap length δ is 6.0 mm. When lower guide-rollers contact with the guideway, the airgap lengths at the front and rear are 1.6 mm and 1.8 mm respectively. Therefore, the possible pitching-angle limited by guide rollers is about -0.263 deg$\sim$0.251 deg.

3. Decoupled Control of Attractive-normal and Thrust Forces in a SLIM Based on FEM Analysis

Decoupled control method of attractive-normal and thrust forces in a SLIM was derived based on analytical formulas.[8] And it was verified by levitation-propulsion control experiment that the SLIM Maglev vehicle could be levitated and propelled by SLIM only.[10),11] But to derive decoupled control, the short primary end effect was neglected and only fundamental forward-travelling current was considered.

In this paper, attractive-normal force in a SLIM is analyzed by FEM to control the vehicle accurately in the levitation direction. Moreover, decoupled control method of attractive-normal and thrust forces based on FEM is derived.

3.1 Attractive-normal force in a SLIM based on FEM

In the FEM analysis, instantaneous values of primary current are expressed as follows :

$$i_u=\sqrt{2}I_1\cos(\theta) \quad (1)$$

$$i_v=\sqrt{2}I_1\cos(\theta-2\pi/3) \quad (2)$$

$$i_w=\sqrt{2}I_1\cos(\theta-4\pi/3) \quad (3)$$

Figure 3 shows the attractive-normal force by FEM and analytical formula at the airgap length of 4.0 mm. It is found that attractive-normal force by FEM changes depending on the phase of primary current.[13] It is also found that attractive-normal force by FEM is the maximum value with $\theta=60$ deg, 240 deg, which correspond with the normal force by analytical formula, and attractive-normal force is the minimum value with $\theta=150$ deg, 330 deg as shown in **Fig. 3**.

3.2 Formularization of attractive-normal force

Attractive-normal force is formularized from **Fig. 3**. Attractive-normal force F_z can be expressed by using F_{z0} which is attractive-normal force by analytical formula as follows :

$$F_z=F_{z0}/(a_0+a_1\theta+a_2\theta^2+a_3\theta^3) \quad (4)$$

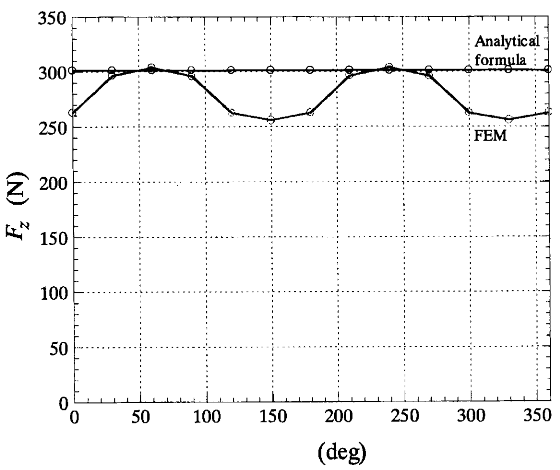

Fig. 3 Attractive-normal force by FEM and Analytical formula ($\delta=4.0$ mm, $I_1=13.4$ A)

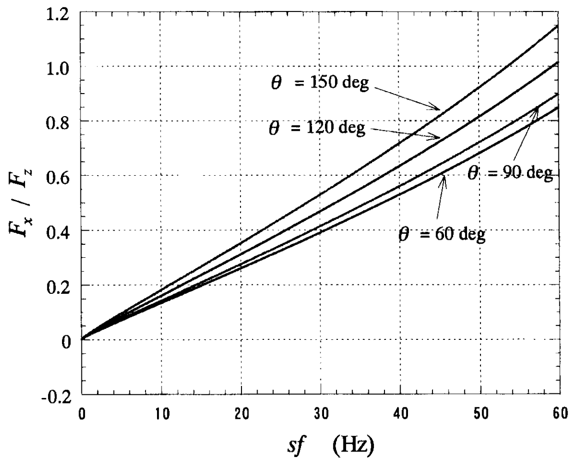

Fig. 4 F_x/F_z depending on only sf for θ

F_{z0} can be expressed as a function of effective value of primary current I_1, and slip-frequency sf.[8]

Therefore, normal force can be expressed as follows :

$$F_z=f_z(I_1, sf, \theta) \quad (5)$$

3.3 Decoupled Control

By analytical formula, thrust force can be expressed as a function of effective value of primary current I_1 and slip-frequency sf as follows[8] :

$$F_x=f_x(I_1, sf) \quad (6)$$

Figure 4 shows F_x/F_z depending on only sf for θ. From **Fig. 4**, it is found that sf is determined uniquely for arbitrary F_x/F_z because θ can be calculated from frequency f. To calculate sf from F_x/F_z, sf is expressed as a function of F_x/F_z and θ by an approximate calculation as follows :

$$sf=b_0\times\frac{F_x}{F_z}+b_1\times\left(\frac{F_x}{F_z}\right)^3 \quad (7)$$

Where b_0 and b_1 are a function of θ.

Then from eq. (6) , I_1 can be calculated as follows :

$$I_1=f_{I_1}(F_z, sf, \theta) \quad (8)$$

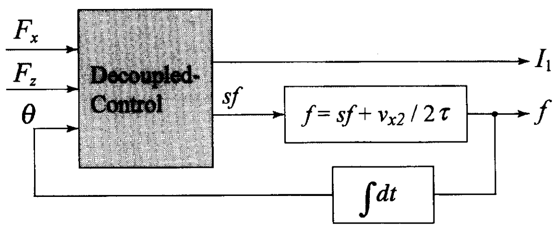

Fig. 5 Block diagram of decoupled control of attractive-normal and thrust forces in a SLIM based on FEM analysis

Figure 5 shows the block diagram of decoupled control of attractive-normal and thrust forces in a SLIM based on FEM analysis. Because θ can be calculated from frequency f, I_1 and sf are determined uniquely for arbitrary F_x and F_z.

4. Control system

4.1 Compensation for lag of gapsensor

In experiments, a laser sensor is used as a gapsensor. To realize a stable levitation of the vehicle, the vehicle must be responded quickly to the guideway vibration. Therefore, the lag of the gapsensor must be considered. Response speed of the gapsensor is 5 ms. **Figure 6** shows the step response of the laser sensor.[14] By using the first order lag element, this lag is expressed as follows :

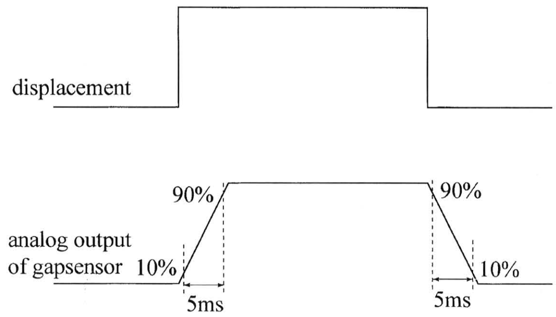

Fig. 6 Step response of gapsensor

$$G(s) = \frac{1}{Ts+1} \tag{9}$$

To compensate for this lag, estimated airgap length is obtained as follows :

$$\hat{\delta} = \{1/\hat{G}(s)\} \times G(s)\delta \tag{10}$$

$1/G(s)$ can be expressed in discrete-time system as follows :

$$1/\hat{G}(s) = 1 + \hat{T}s \rightarrow$$

$$1 + \hat{T} \cdot \frac{1-z^{-1}}{ts} = 1 + k(1-z^{-1}) = 1/G(z) \tag{11}$$

Therefore, estimated airgap length is calculated as follows :

$$\hat{\delta}_n = \delta_n + k(\delta_n - \delta_{n-1}) \tag{12}$$

where δ_n is the nth measured value of gapsensor and δ_{n-1} the $(n-1)$th measured value of gapsensor.

4.2 Block Diagram

Figure 7 shows the block diagram of control system for SLIM experimental Maglev vehicle. Ac-

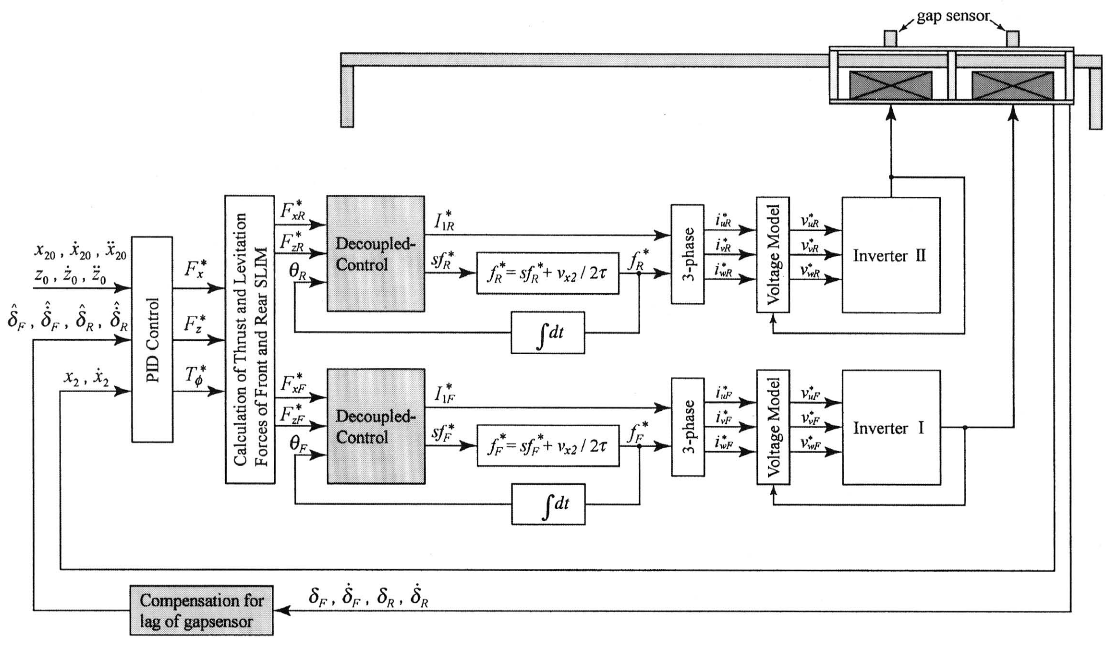

Fig. 7 Block diagram of control system for SLIM experimental Maglev vehicle

cording to the optimal robust servo control theory, to follow quickly the demand patterns of vehicle position x_{20} and levitation height z_0 and to restrain the pitching motion, command thrust force F_x^*, normal force F_z^* and pitching torque T_ϕ^* are determined. Then, from the command normal force F_z^*, thrust force F_x^* and pitching torque T_ϕ^*, command normal forces F_{zF}^*, F_{zR}^* and the command thrust forces F_{xF}^*, F_{xR}^* of the front and rear SLIM are calculated. Command slip-frequency sf_F^* of the front SLIM is calculated from eq. (7). Then command effect value of armature-current of front SLIM I_{1F}^* can be calculated from F_{zF}^*, sf_F^* and demand airgap length δ_F. In addition, command frequency f_F^* can be also determined from considering sf_F^* together with the vehicle speed v_{x2}. Similarly, sf_R^*, I_{1R}^*, f_R^* are determined. In brief, for arbitrary F_x^*, F_z^* and T_ϕ^*, I_{1F}^*, f_F^*, I_{1R}^* and f_R^* can be determined uniquely and the vehicle can be levitated by normal force and propelled by thrust force in the SLIM.

The sampling time of motion control is 0.5 ms and the sampling time of the current control is 0.1 ms.

5. Experiment

In the experiment, an initial airgap length is 6 mm with upper guide-roller contacting with the guideway. The vehicle is first levitated upward from airgap length 6 mm to 4 mm at standstill at a place where the center of the vehicle is 78 cm away from the end of the guideway, and then is driven until 1.5 m along the guideway at the maximum speed of 0.1 m/s between two pillars. After that, the vehicle is controlled to land at standstill.

Figure 8 shows the experimental results of combined-levitation-propulsion SLIM Maglev vehicle. As shown in **Fig. 8** (a) and (b), vehicle position x_2 and speed v_{x2} were controlled very well to follow the demand pattern x_{20} and v_{x20}. **Figure 8** (c) shows the front and rear airgap lengths δ_F, δ_R. The vehicle was propelled with small vibration, and this vibration was within about ±0.5 mm for demand airgap length of 4.0 mm. **Figure 8** (d) shows the pitching angle ϕ. When the vehicle took off, the maximum pitching angle was 0.14 deg. And when the vehicle was propelled, pitching angle was within ±0.05 deg. It is found that the vehicle was propelled and levitated without contacting the guideway from **Fig. 8** (c) and (d). **Figure 8** (e), (f) show the command levitation forces of the front and the rear SLIM F_{zF}^*, F_{zR}^* and T_ϕ^*. **Figure 8** (g), (h) show the command effective values of primary current of the front and rear SLIM I_{1F}^*, I_{1R}^* and measured instantaneous values of u-phase current of front and rear armature i_{uF}, i_{uR}.

6. Conclusions

In this paper, we have presented a combined-levitation-and-propulsion control system of SLIM Maglev vehicle which can correspond quickly and accurately to the vibration of the guideway based on the analyzed attractive-normal force. Combined-levitation-and-propulsion control experiment has been carried out successfully by the proposed control system including the accurately estimated airgap length which is easily calculated every 0.5 ms from the measured airgap length by gapsensor.

References

1) K. R. Davey : "Transverse Flux Linear Induction Motors Applied to Magnetic Suspension System", Proc. of 6th ISMST, Vol. 1, pp. 228-232, (2002-10).
2) S. Suzuki, M. Kawashima, Y, Hosoda and T. Tanida : "HSST-03 System", IEEE Transactions on Magnetics, **MAG-20**, No. 5, pp. 1675-1677, (1984-9).
3) K. Yoshida : "Magnetic Levitation and Linear Motor, Science of Machine, **42**, No. 4, pp. 468-474, (1990).
4) K. Yoshida and S. Nagao : "Levitation and Propulsion Control and Simulation of Superconducting LSM Maglev Vehicle", Report of LD-90-63 of the Joint Studying Committee on Magnetics and Linear Drives, pp. 39-48, (1990).
5) K. Yoshida and S. Nagao : "Levitation and Propulsion Control Simulation of Regardless-of-speed Superconducting LSM Repulsive Maglev Vehicle", Proc. of the 3rd Electromagnetics Symposium, pp. 201-206, (1991).
6) K. Yoshida, H. Takami and L. Shi : "Decoupled-Control of Levitation and Propulsion in Underwater LM car ME02", the Journal of Mathematics and Computers in Simulation, **46**, pp. 239-256, (1998).
7) K. Yoshida, H. Takami and N. Shigemi : "Repulsive-Mode Levitation and Propulsion Control of a Land Travelling Marine-Express Model Train ME03", Proc. of LDIA'95 Nagasaki, pp. 41-44, (1995-6).
8) K. Yoshida, L. Shi and T. Yoshida : "A Proposal of Decoupled-Control of Attractive-Normal and Thrust Forces in a SLIM for Maglev Vehicle", Proc. of the 6th International Conference ELECTRIMACS, pp. 221-226, (1999-9).
9) K. Yoshida and S. Nonaka : "Levitation Forces in Single-Sided Linear Induction Motors for High-speed Ground Transport", IEEE Transactions on Magnetics, **MAG-11**, No. 6, pp. 1717-1719, (1975-11).
10) K. Yoshida, T. Yoshida, K. Hayashi and H. Takami : "Decoupled Control of Levitation and Propulsion in SLIM Experimental Maglev Vehicle, Proc. of ICEM, Vol. 1, pp. 228-232, (2000-8).
11) K. Yoshida, T. Yoshida and K. Hayashi : "Combined Lev-

itation and Propulsion Control in a SLIM Experimental Maglev Vehicle", Proc. of 6th ISMST, Vol. 1, pp. 404-409, (2001-10).

12) K. Yoshida and T. Yoshida : "Standstill Levitation Control in a Combined Levitation-Propulsion SLIM vehicle, taking into account flexure of the guideway", National Conventional Record I.E.E Japan, vol. 5, p368, (2001-3).

13) K. Yoshida, T. Yoshida and K. Noda : "Influence of end effects on attractive levitation force at standstill in combined-levitation-and-propulsion SLIM", Record of Joint Conference of Electrical and Electronics Engineering in Kyushu, p. 125, (2002-9).

14) "Lasor Displacement Sensor Users Manual", Omron Co. Ltd.

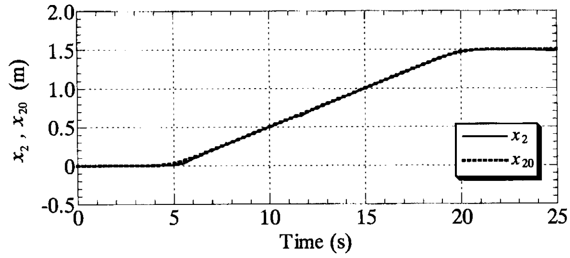

(a) Demand and measured vehicle positions

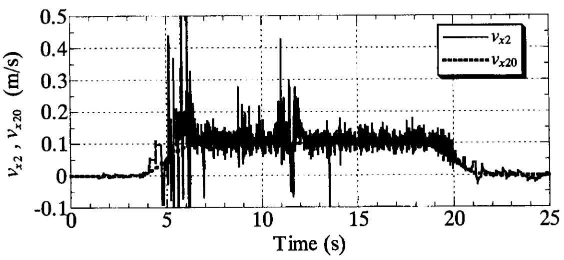

(b) Demand and measured vehicle speeds

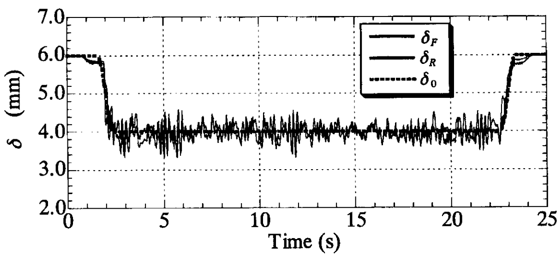

(c) Demand and measured airgap lengths at front and rear

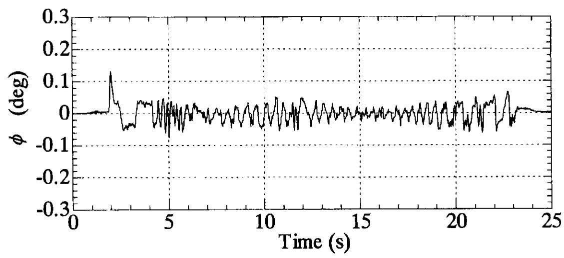

(d) Measured pitching angle

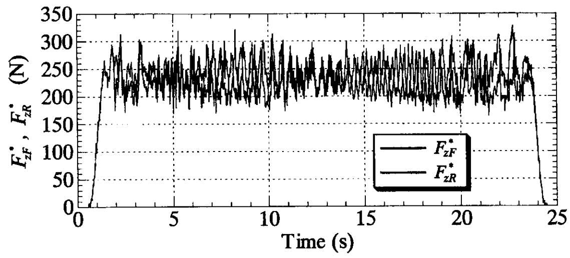

(e) Command levitation forces of front and rear SLIM

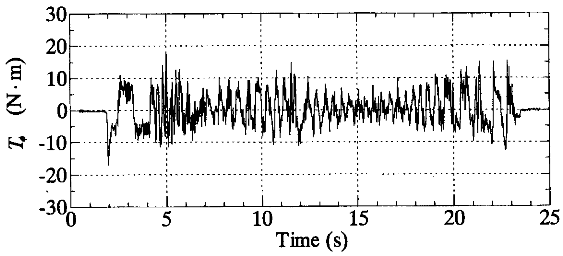

(f) Measured pitching torque

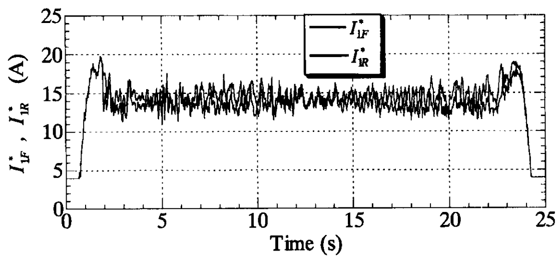

(g) Command effective values of primary current of front and rear armature

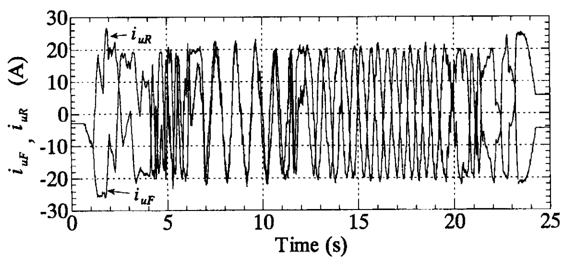

(h) Measured instantaneous values of u-phase current of front and rear armature

Fig. 8 Experimental results of combined-levitation-and-propulsion control in SLIM Maglev vehicle